

---

## **GEO-ELECTRIC INVESTIGATION OF GROUNDWATER POTENTIAL IN LADERIN HOUSING ESTATE, ABEOKUTA, SOUTHWESTERN, NIGERIA**

**<sup>1</sup>A. A. ALABI , <sup>2</sup>A. O. ADEWALE, <sup>1</sup>O.O. ADELEKE, <sup>1</sup>F. G. AKINBORO,  
<sup>1</sup>AYODEJI AFE AND <sup>1</sup>ADAM GANIYU**

<sup>1</sup>Department of Physics, Federal University of Agriculture, Abeokuta, Nigeria

<sup>2</sup>Department of Science Laboratory Technology, Moshood Abiola Polytechnic Abeokuta, Nigeria.

\*Corresponding Author: derylab@yahoo.com Tel: +2348035810262

---

### **ABSTRACT**

Vertical Electrical Sounding (VES) and 2D Electrical Resistivity Tomography (ERT), with Schlumberger and Wenner electrode array configurations respectively were employed to investigate the groundwater potential of Laderin Housing Estate located at Oke-mosan, Abeokuta, Ogun state, southwestern Nigeria. The area is underlain by the basement complex of the southwestern Nigeria. The research aimed at determining the aquifer/groundwater zone and characterizes the lithology of the study area. The geophysical survey involving nine VES and four profile of 2-D ERT lines with lengths varying from 100 m to 150 m were carried out. The field data from both the ERT and VES were processed and interpreted using RES2DINV and WINRESIST software respectively. Geometrical effects from the pseudo-section were removed and an image of true depth and true formation resistivity were produced. Three to four geo-electric layers were revealed in all, which are; topsoil, weathered layer, fractured and fresh basement rock. The result of 2 D inversion provide lithologic unit, weathering profile and geological structure favourable for groundwater potential. The results show that the basement rock was delineated with resistivity values that range between 701.3  $\Omega\text{m}$  and 9459.3  $\Omega\text{m}$ . The bedrock topography has a variable thickness of overburden between 3 m and above 16.4 m, which is fairly shallow. The geophysical survey show that VES 2, VES 3, VES 4, VES 5, and VES 6 are possible location for groundwater extraction. The difficult terrain, where thick overburden are located are also promising target for groundwater development.

**Keywords:** resistivity; groundwater potential; weathering profiles; geo-electric layers; aquifer

### **INTRODUCTION**

Water occurs naturally on the earth's surface as streams, rivers, oceans, lakes springs and beneath the earth's surface as groundwater. Water is basic ware for the survival of all living things (plants and creatures). The total amount of water in rivers, ocean and lakes that are accessible for human usage is

less than 0.08% of global fresh water reserve (Anomohanran, 2013). Groundwater is preserved water found in the subsurface of the earth as underground streams and in aquifers. Groundwater has become popular source of potable water in Nigeria because of its quality and consistent availability compared to other sources of water. Groundwa-

ter is known to be free from pollutants most times and requires next to zero disinfecting before usage. Groundwater is usually free from odour, colour and has a very low dissolved solid (Lawrence and Ojo, 2012).

The geophysical methods, which include; seismic, magnetic, electrical resistivity, induced polarization and electromagnetic techniques employ the application of the principles of physics to study the shallow or deep features of the earth's crust, which vary in respect of physical properties of rocks such as rock density, dielectric constant, resistivity and susceptibility (Okafor, 2011). Ayolabi *et al.* (2009) applied seismic refraction to investigate structural settling of subsurface materials and groundwater potential in Igbogbo Township. Aquifer characteristics and formation layers of the location were delineated. Lawrence and Ojo (2012) employed a low frequency electromagnetic and the electrical resistivity methods to evaluate the aquifer potential of a typical basement complex terrain of Ado – Ekiti in Nigeria. The electrical resistivity technique has been the most frequently employed geophysical method for groundwater investigation because of its simplicity in application and interpretation (Anomohanran, 2013). Electrical resistivity techniques are efficiently applied for groundwater investigation in the region where there is electrical resistivity contrast between the water bearing and the fundamental rocks (Jayeoba and Oladunjoye, 2015). Sharma and Baranwal (2005) employed electrical resistivity techniques to investigate groundwater potentials. Sounding and profiling technique, gives 1-D model of the subsurface, which is not a sufficient method for mapping areas of complex subsurface geology. Assumption of hori-

zontally stratified earth model during interpretation may not always be true for most local geological model and inability of the profiling method to note changes in measured resistivity with respect to depth, contributed to limitation of these methods (Griffiths and Barke, 1993). Electrical Resistivity Tomography offers a more accurate 2-D resistivity model of the subsurface, where resistivity changes in the horizontal and in the vertical direction along the survey line are mapped continuously without been affected by the presence of geological and topographical complexities (Loke, 2000). The 2-D Electrical resistivity tomography technique has been a ground-breaking method in examining shallow subsurface electrical structures in different locations (Yang *et al.*, 2002; Hauck *et al.*, 2003; Cheng *et al.*, 2008; Crook *et al.*, 2008). Various Studies (Zhou *et al.*, 2004; Hsu *et al.*, 2010 and Rao *et al.*, 2013) have employed 2D electrical resistivity tomography in geological mapping, bedrock detection and groundwater investigation. The availability of groundwater is affected by the extent and depth of weathering and fracturing. The groundwater is primarily recharged by surface precipitation and also through horizontal flow from rivers.

Laderin housing estate and its environs is a rapidly developing residential estate along the newly dualized, Abeokuta, Shagamu expressway, Oke – Mosan, Abeokuta, Ogun state, Nigeria, situated in the basement complex of southwestern Nigeria. The area had suffered a serious setback on groundwater exploration and exploitation over the years. Since surface water is exposed to several kinds of abuse, groundwater remains the only reliable source of water supply that could be developed to reduce problems of long trek of distances by women and children in search for water during the dry sea-

son. The uneven distribution of groundwater in space, time and circulation (Ajayi and Adegoke, 1988) suggest necessity to embark on groundwater survey before borehole could be drilled. In this study, hydrogeological characterization of the area was conducted by employing VES and 2D electrical resistivity tomography methods to enhance proper planning for the exploration and exploitation of groundwater resources in

the estate.

## MATERIALS AND METHODS

### *Site Description and Geological Settings*

The study area is located on latitude  $07^{\circ}07'8.0''$  and  $07^{\circ}07'28.0''$  and longitude  $03^{\circ}23'12.0''$  and  $03^{\circ}23'26.0''$  which is along Shagamu-Abeokuta express road (Figure 1).

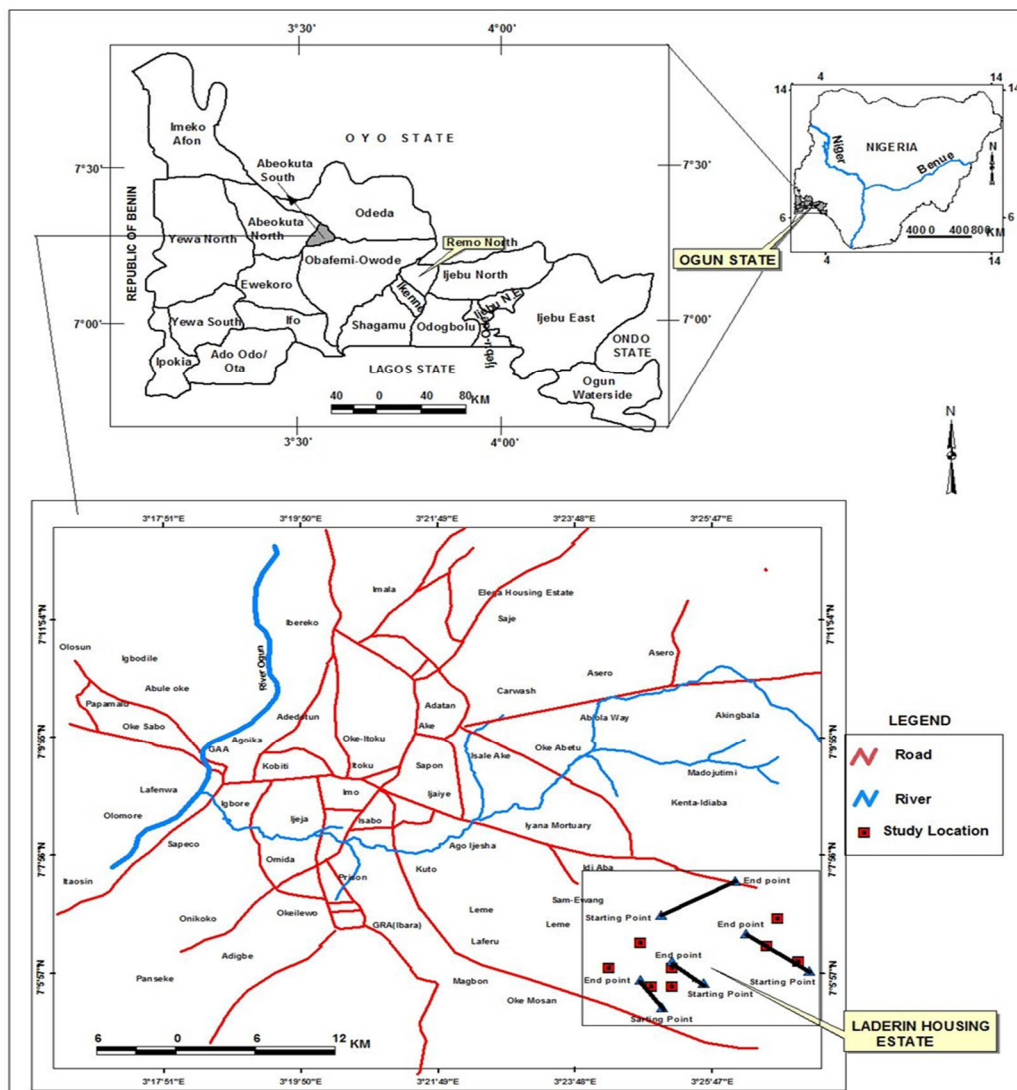


Figure 1: Map of the study area

The study area is underlain by crystalline rocks of Precambrian Basement Complex of Southwestern Nigeria (Figure 2), which comprise of folded gneiss, schist, quartzite, older granite and amphibolites/mica schist (Jones and Hockey, 1964; Rahman, 1989).

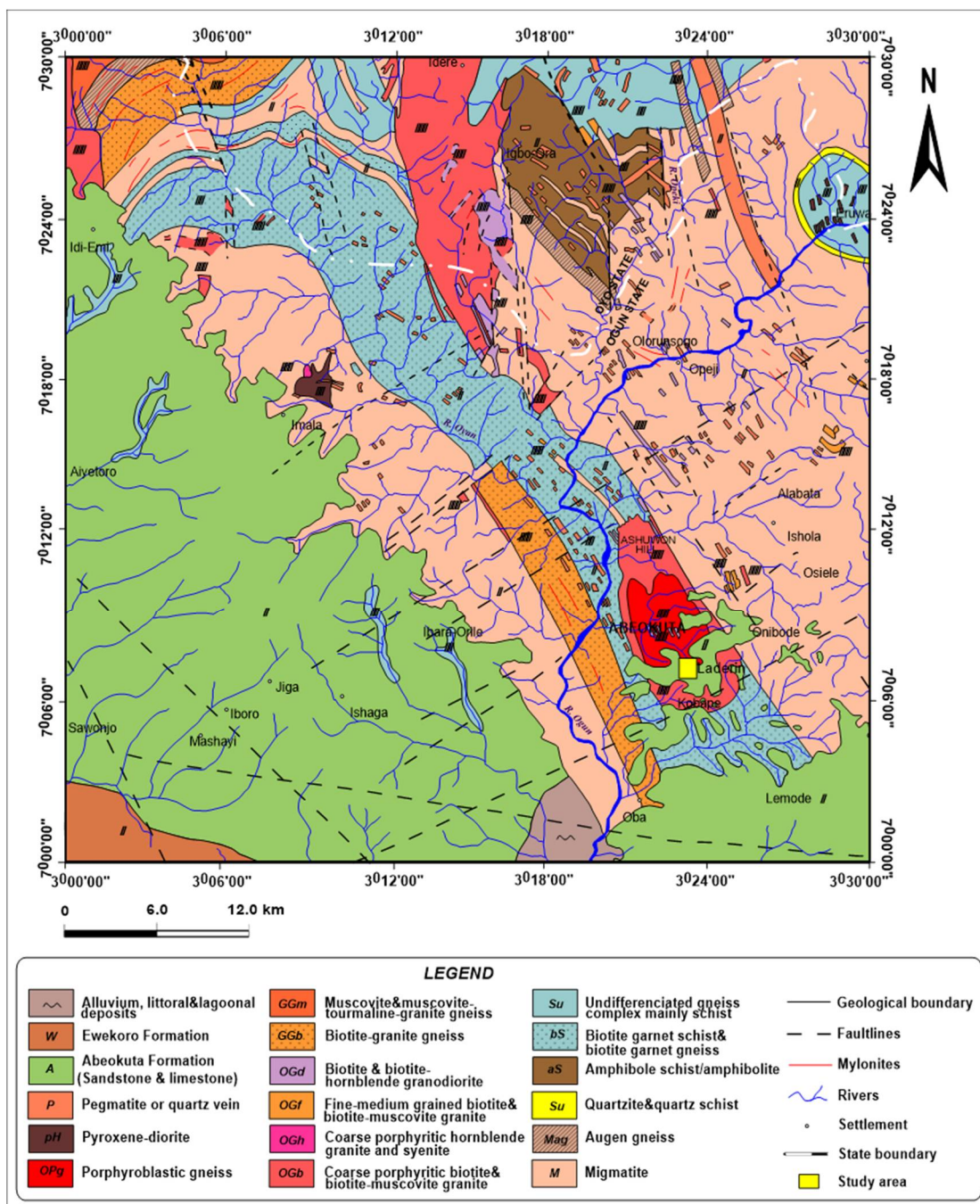


Figure 2: Geological Map of the study area

Laderin has a tropical rainy and dry season with a long rainy season and moderately steady temperatures span through the year. The rainy season covers March to October while the dry season spans through November to February. The mean aggregate precipitation is 1420.06 mm with two pinnacles of precipitation in June and September. The mean maximum temperature is 26.46 °C,

while the least temperature is 21.42 °C and the relative humidity is 74.55 % (NIMET, 2011). The study area is underlain by Precambrian basement complex rock of southwestern Nigeria.

The geographic coordinates of the VES stations and the Wenner profiles were obtained (Figure 3).

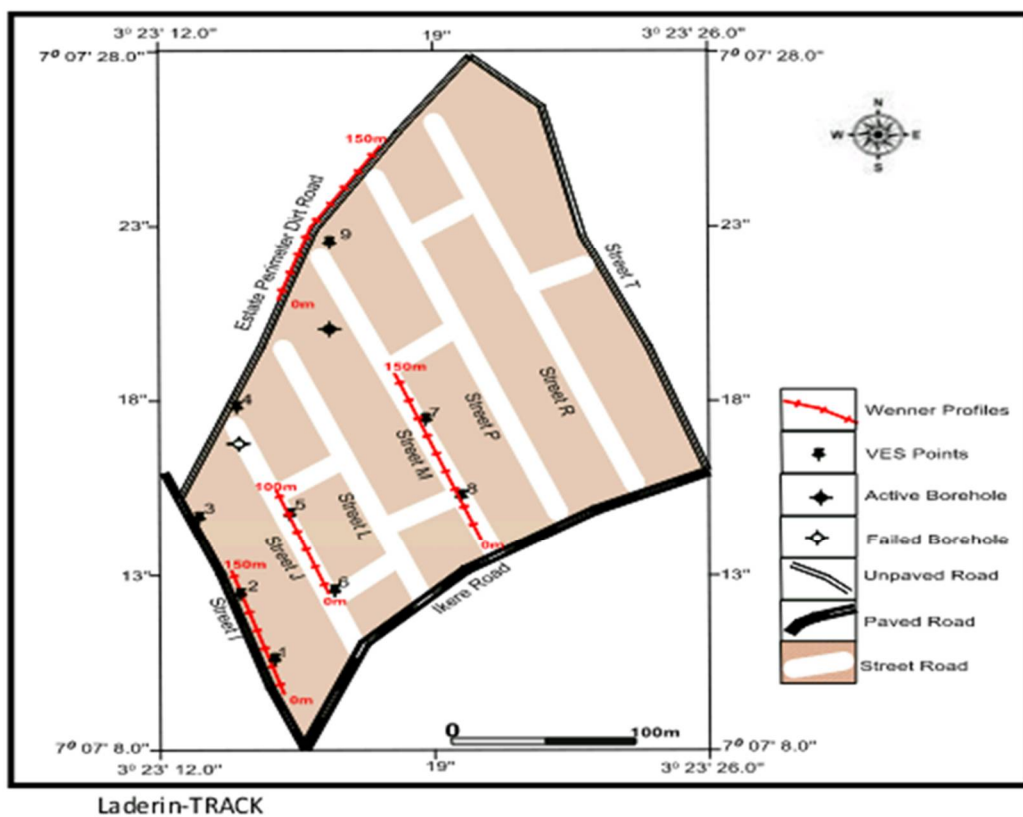


Figure 3: Location map of the VES points and Wenner profiles

**Field Procedure, Data Acquisition and Presentation**

Electrical imaging is an appropriate method for complex geology region particularly where the resistivity sounding and other techniques have not been providing comprehensive information about the subsurface properties of an area (Barker, 1999).

Nine VES data points were conducted within the study area using an OHMEGA resistivity meter. The Schlumberger electrode array was adopted with a maximum electrode spread  $\frac{AB}{2}$  of 100 m and profile length ranging from 100 m to 150 m. Though

Schlumberger array is better when focusing on groundwater potential because it is less sensitive to lateral resistivity variation, slightly faster in field operation and involves minimal labour cost than other configurations, this research work employ Wenner configuration in addition for comprehensive results. In Schlumberger configuration four electrodes were employed, with two electrodes been current electrode (C1 and C2) and the other two electrodes were Potential electrodes (P1 and P2) as shown in figure 4. The current electrodes were spaced much

further apart than the potential electrodes. The current electrodes were move outward symmetrically about the centre of the spread and the potential electrode separation was kept constant. The electrode spread of  $AB/2$  was varied from 1 to a maximum of 100 m. Sounding data were presented as sounding curves, by plotting apparent resistivity against  $AB/2$  or half the spread length on a bi-log graph. The Geo-electric factor  $K$  and the apparent resistivity were then calculated.

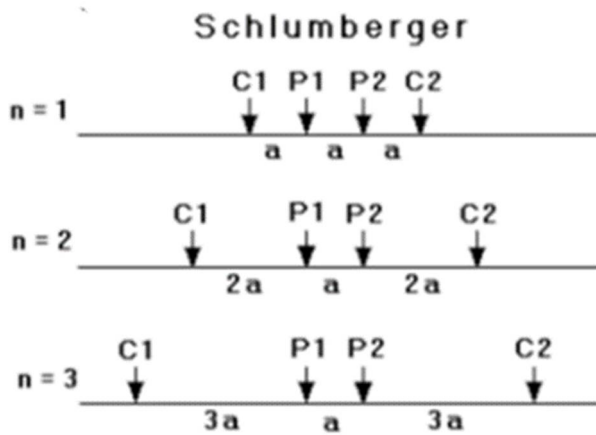


**Figure 4: Schlumberger Array (Loke, 2004)**

Electrical resistivity 2-D imaging using Wenner array was also applied to conduct four profiles. A leveled terrain was located as the Wenner station, the four electrodes were positioned symmetrically along a straight line of which the current electrodes (C1 and C2) are on the outside and the potential electrodes (P1 and P2) are the inner electrodes place in between C1 and C2 with equal distance of 5 m between each of the electrode. The resistivity meter was powered

by DC source and further adjustments such as; automatic reading of values in Ohms and sending a 50 mA of current into the ground were made on it. The four electrodes were moved simultaneously at the same time with 5 m distance from the previous point and maintaining the same distance between the electrodes. The initial distance between the electrodes before the data was collected was 5 m then it was increased to 10 m, 15 m, 20

m and 25 m which follows the pattern in figure 5 where  $a = 5$ .

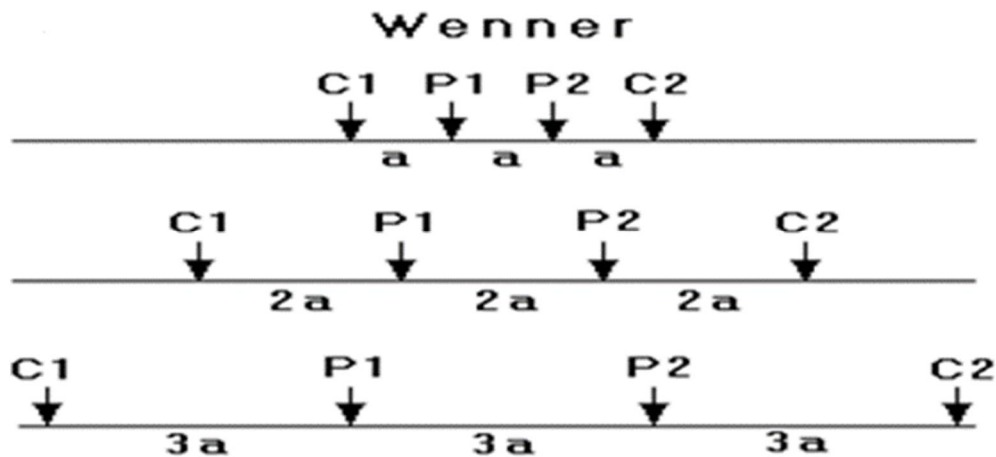


**Figure 5: Wenner Array (Loke, 2004)**

The values of resistivity obtained in the field were multiplied with their respective geometric factor ( $k$ ).

The field work was carried out in August, a period that falls within the rainy season in the study area, when the ground was considerably moist. The moisture enhanced flow of current within the earth and the electrodes, although it was generally necessary to carry out the electrical resistivity work when the ground is relatively moist (Sundaravaradan and Reddy, 2018), the survey work was not carried out on the day when there was down pour as water logged soil may result to enormously high conductivity near the ground surface. The resistivity meter usually displays negative resistance when current signal to the ground is insufficient, at such stages the instrument would be adjusted to high current signals. Some precautions were taken when the research was conducted in the field, these include

avoidance of locating the sounding points in the vicinity of known buried conductors since the presence of buried pipeline cables and other metallic conductors could constitute electrical noise to the field data. A well-insulated and light weighted wires of very low resistance were used in connecting electrodes and the resistivity meter; such wires ensure high quality insulation since leakage between the current circuit and the measuring circuit is one of the primary sources of errors in resistivity measurement (Keller and Frischknecht, 1966). Low resistant wires are used because high resistance wires significantly affect the measured resistance, especially if it connects the potential electrodes.

The curve matching and computer iterative modelling methods of interpretation were applied to VES data. The apparent resistivity was plotted against the half electrode spacing using bi logarithmic (log-log) transparent paper. The various points were joined to give

a VES curve. The VES curves were compared with collection of standard graphs (model curves), which have been pre-calculated for assumed multilayer resistivity profiles. The superimposition of the VES curve over the theoretical curves yields values of thickness, depth and resistivity value for the geo-electric area in the study area. The results obtained from the curve matching method (resistivity, thickness and number of layers) were employed as a starting parameter for the model in WINRESIST software. The software generated a set of theoretical apparent resistivity comparable with the result obtained from the field and the curve. The layer parameters are automatically adjusted by the software, if no match (fit) is obtained. The noisy data points from the four Wenner stations at different electrodes spacing were filtered, processed and inverted using RES2DINV. The inversion of the data was done to estimate the true resistivity of the subsurface by finite element forwarding (Geo-Etude, 2003). The large resistivity variations near the ground surface were taken care of by model refinement option of the inversion menu.

## RESULTS AND DISCUSSION

### *Vertical Electrical Sounding Results*

The data acquired from the nine soundings revealed three to four layers, of which five are A- and four are H-type (Table 1). The topsoil was made up of layers with resistivity values ranging from 54 to 441.1 ohms-m indicating that the topsoil was mainly sandy to lateritic in nature, with thickness of 0.53 to 2.5 m. The clay layer resistivity ranged

from 51.9 to 440 ohm-m and having a thickness of about 1.3 to 3 m. The weathered basement layer resistivity varied from 164 to 498.1 ohm-m and having thickness of about 3.6 to 15.2 m. In respect of hydro-geology, the weathered layer had significance groundwater, where it was thick enough and the amount of water saturating it was high.

The fractured layer was delineated beneath three VES points: 1, 6 and 9. The layer constitutes main aquifer unit in the study area and resistivity falls between 664.9 and 957.7 ohm-m. The fresh basement was made up of the layer with resistivity ranging from 1231.1 to 9459.3 ohm-m. This high resistivity was due to the crystalline nature of the study area.

### *Geoelectric Section*

Electrical resistivity methods enable the determination of subsurface resistivity variations in the ground resistivity that exist across geo-electric boundaries in the subsurface. The two dimensional view of the geo-electric parameters (resistivity and thickness) obtained, were employed in determining aquiferous or non-aquiferous layer and reliable geological deductions. The geo-electric sections (figures 14 to 17) of the various VES stations in the study area were constructed to depict different geo-electric layers. The geo-electric sections obtained in the area were indicated as AA, BB, CC and DD.



**Table 1:** Summary of coordinates, resistivity, thickness, depth, probable lithology and curve

VES No	Coordinates	Elevation (m)	Layer Resistivity ( $\Omega\text{m}$ )	Thickness (m)	Depth (m)	Probable Lithology	Curve Type
1	7°7'19.9" 3°23'18.6"	163	145.3	2.5	2.5	Topsoil	A
			440.6	3	5.5	Lateritic Clay	
			664.8			Weathered Bedrock Fresh Bedrock	
2	7°7'12.0" 3°23'14.2"	164	441.1	0.3	0.3	Topsoil	H
			164.1	5	5.3	Weathered Bedrock Fresh Bedrock	
3	7°7'14.1" 3°23'13.0"	167	1231.1			Topsoil	A
			152.2			Lateritic Clay	
			211.3 2220.9			Weathered Bedrock Fresh Bedrock	
4	7°7'17.1" 3°23'13.8"	151	140.1	0.7	0.7	Topsoil	H
			66.4	1.3	2	Weathered Bedrock Fresh Bedrock	
5	7°7'14.2" 3°23'15.0"	161	2216.1			Topsoil	A
			103.0			Lateritic Clay	
			164.4 1402.2			Weathered Bedrock Fresh Bedrock	
6	7°7'12.1" 3°23'15.0"	167	69.7	0.5	0.5	Topsoil	H
			51.9	1.4	1.9	Weathered Bedrock Fresh Bedrock	
7	7°7'16.8" 3°23'18.4"	160	957.7			Topsoil	A
			89.1	2.3	2.3	Lateritic Clay	
			498.1 1545.4	3.6	5.9	Weathered Bedrock Fresh Bedrock	
8	7°7'14.7" 3°23'19.2"	165	73.2	1.2	1.2	Topsoil	H
			475.2	15.2	16.4	Weathered Bedrock Fresh Bedrock	
9	7°7'14.5" 3°23'15.2"	163	2516.4			Topsoil	A
			54.0	0.4	0.4	Lateritic Clay	
			701.3 9459.3	11.2	11.6	Weathered Bedrock Fresh Bedrock	

**Geoelectric Section**

Electrical resistivity methods enable the determination of subsurface resistivity variations in the ground resistivity that exist across geo-electric boundaries in the subsurface. The two dimensional view of the geo-electric parameters (resistivity and thickness) obtained, were employed in determining aquiferous or non-aquiferous layer and reliable geological deductions. The geo-electric sections (figures 14 to 17) of the various VES stations in the study area were constructed to depict different geo-electric layers. The geo-electric sections obtained in the area were indicated as AA, BB, CC and DD.

**Geo-electric Section AA**

The geo-electric section AA made up of data from VES 8, 7, and 9 (figure 6). The interpretative cross sections AA show three geo-electric layers. The topsoil which is characterized by resistivity values ranging from 54  $\Omega\text{m}$  to 89  $\Omega\text{m}$  with thickness varies from 0.4 m to 2.3 m. The second layer has a resistivity value varies from 475  $\Omega\text{m}$  to 701  $\Omega\text{m}$  with thickness varies from 1.3 m 11.2 m and is presumed to be weathered bedrock. The third layer has a resistivity value that varies from 1545  $\Omega\text{m}$  to 9459  $\Omega\text{m}$  and is presumed to be fresh basement.

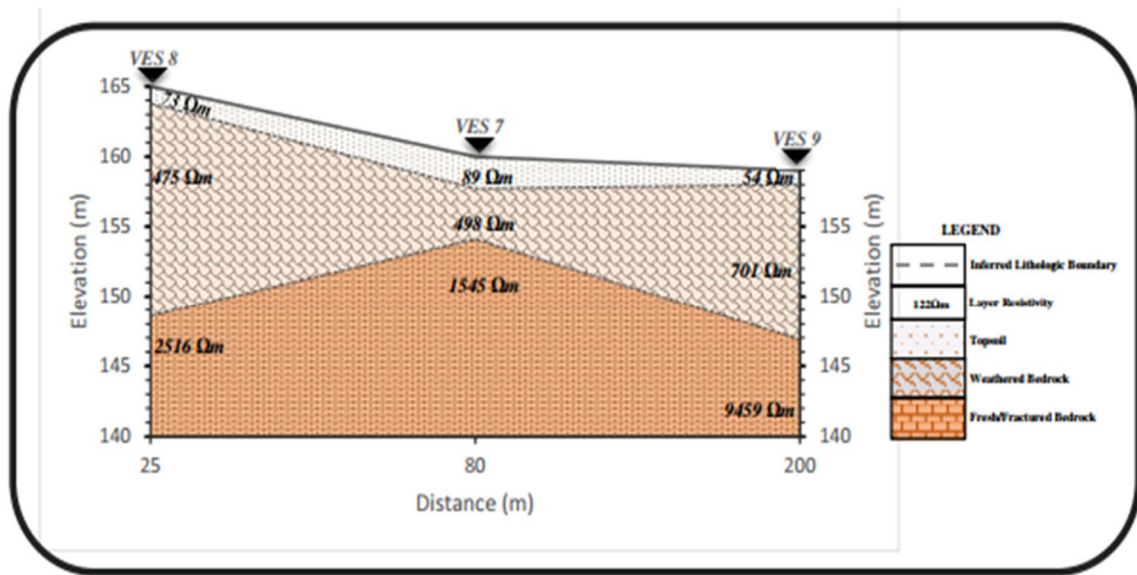
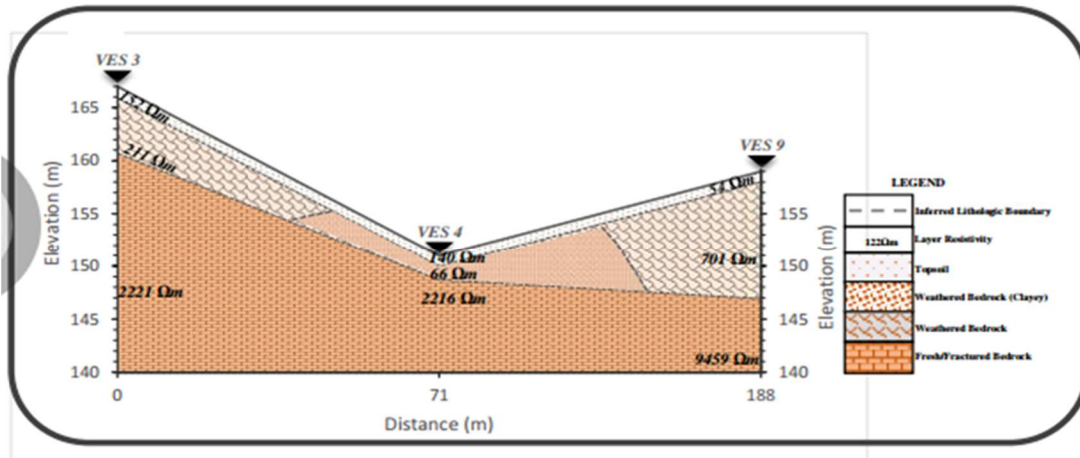


Figure 6: Geo-electric section AA across VES 8, 7 and 9

**Geo-electric Section BB**

The geo-electric section BB is made up of VES 3, 4, and 9 (figure 7). The interpretative cross sections BB show three geo-electric layers but four geological substances. The topsoil is characterized by resistivity values ranging from 54  $\Omega\text{m}$  to 152  $\Omega\text{m}$  with thickness varies from 0.4 m to 1.1 m. The

second layer has a resistivity value that varies from 66  $\Omega\text{m}$  to 701  $\Omega\text{m}$  with thickness varies from 1.3 m to 11.2 m and is presumed to be clayey weathered bedrock. The third layer has a resistivity value that varies from 1545  $\Omega\text{m}$  to 9459  $\Omega\text{m}$  and is presumed to be fresh/fractured bedrock.



**Figure 7: Geo-electric section BB across VES 3, 4 and 9**

**Geo-electric Section CC**

The geo-electric section CC is made up of data from VES 4, 5, and 6 (figure 8). The interpretative cross sections CC show three geo-electric layers. The topsoil is characterized by resistivity values ranging from 70  $\Omega$  m to 140  $\Omega$  m with elevation that varies

from 160 m to 165 m. The second layer has resistivity values that varies from 52  $\Omega$  m to 164  $\Omega$  m and is presumed to be weathered bedrock. The third layer has resistivity values varies from 958  $\Omega$  m to 2216  $\Omega$  m and is presumed to be fresh/fractured bedrock.

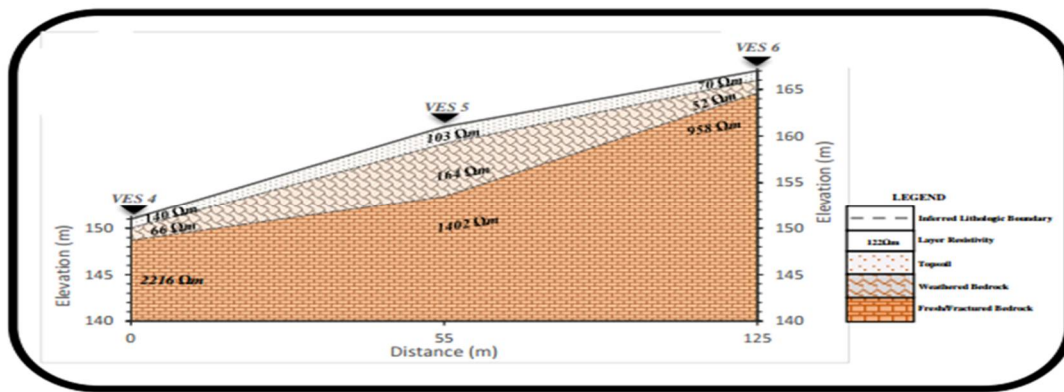


**Figure 8: Geo-electric section CC across VES 4, 5 and 6**

**Geo-electric Section DD**

The geo-electric section DD made up of data from VES 1, 2 and 3 (figure 9). The interpretative cross sections DD show three geo-electric layers. The topsoil is characterized by resistivity values ranging from 145  $\Omega$  m to 441  $\Omega$  m with thickness varies from

0.3 m to 2.5 m. The second layer has resistivity values varies from 164  $\Omega$  m to 441  $\Omega$  m with thickness varies from 3.0 m to 5.1 m and is presumed to be weathered bedrock. The third layer which has resistivity values varies from 665  $\Omega$  m to 2231  $\Omega$  m and is presumed to be fresh/fractured bedrock.

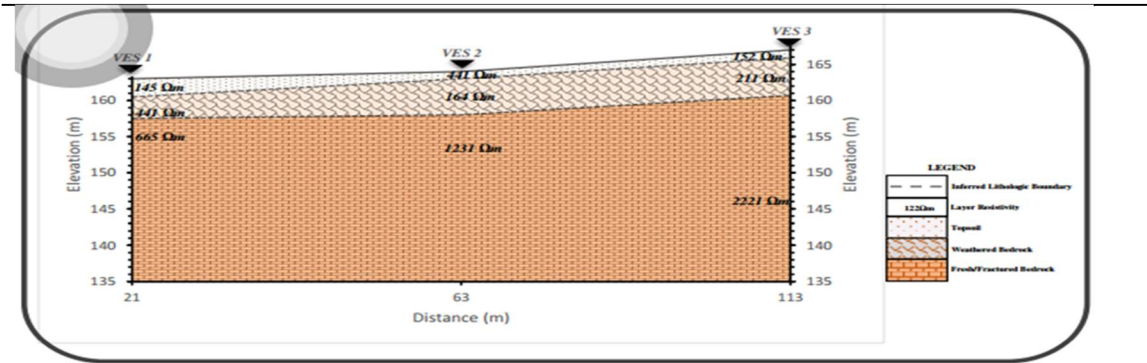


**Figure 9: Geo-electric section DD across VES 1, 2 and 3**

The data set for the 2D-Electrical Resistivity Imaging were processed and inverted using RES2DINV inversion code, which is a non-linear efficient technique for determining 2D resistivity distribution to obtain the profiles.

**Profile 1**

The maximum length of the inverted section of 2-Dimensional imaging of profile 1 data is 150 m (figure 10). The profile reveals topsoil of about 4 m thick with resistivity values ranging from 60 Ωm to 450 Ωm at the southern part of the profile due to the presence of low lying coarse-grained sand. The variation in the resistivity reveals dissimilarity along the topsoil. This layer is underlain by more conductive layer, which

has resistivity value of between 265 Ωm and 450 Ωm and thinned out towards the northern and southern ends of the profile with considerable thickness between 5 m and 8.5 m. The layer is interpreted as clay/clayey sand and under this layer is fractured basement with resistivity values ranges from 500 Ωm to 950 Ωm, which formed the upper section of the basement rock. The fractured basement has uniform thickness of 4.3 m. The base of the profile was occupied by the basement rock that has resistivity value of 3500 Ωm and above. The depth to the basement ranges between 12.5 m and 13.4 m. The uneven thickness across the profile line indicates that there was no uniform weathering across the profile line (Figure 10).

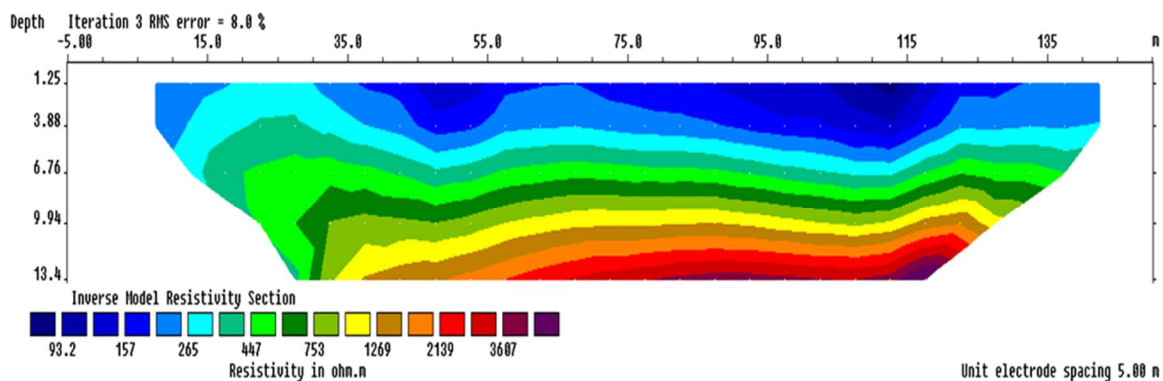


**Figure 10: Inverse model resistivity section for profile 1**

**Profile 2**

The inverted section of 2-Dimensional imaging of profile 2 located at the western part of the study area (Figure 11) trends north-south direction with a length of 100 m. The upper part of the layer revealed conductive materials as the top layer that has resistivity values of between 65  $\Omega\text{m}$  and 117  $\Omega\text{m}$  and is about 3 m thick but absent in lateral distance 15 m to 20 m, 30 m to 35 m and 60 m to 75 m. The top layer was interpreted to be sandy clay. This layer is underlain by a conductive layer, which is about 4 m thick with resistivity values between 120  $\Omega\text{m}$  and 117  $\Omega\text{m}$  and is interpreted as clay/clayey

sand/sandy clay. This layer was present throughout the lateral distance of 100 m where the resistivity of the material is 130  $\Omega\text{m}$  which is interpreted as clayey sand. It coincides with a basement rise. Under this layer is the basement rock with the upper part interpreted as fractured basement, which has resistivity values of between 372 and 850  $\Omega\text{m}$ . The high resistivity values (922  $\Omega\text{m}$  to 1539  $\Omega\text{m}$ ) observed at the depth range from 10 to 13.4 m at the southern part of the section showed that the subsurface materials are resistive and was interpreted as basement rock.

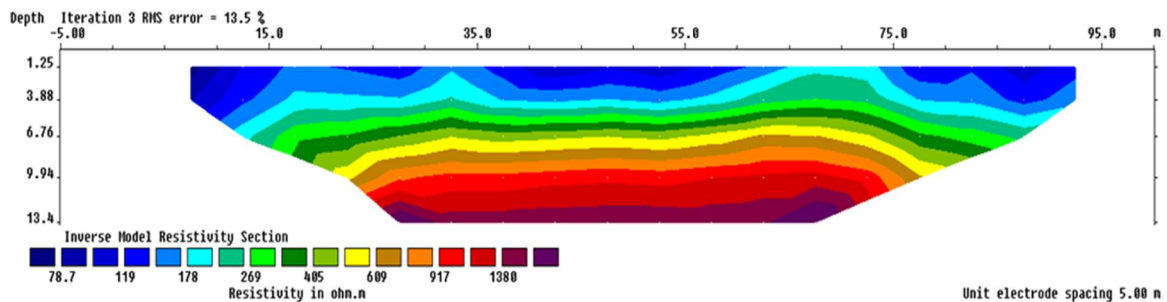


**Figure 11: Inverse model resistivity section for profile 2**

**Profile 3**

The inverted section of 2-Dimensional imaging of profile 3 of the study area trending N-S direction (Figure 12). The maximum length of the profile is 120 m and top layer is about 4 m thick with resistivity values ranging from 100  $\Omega\text{m}$  to 200  $\Omega\text{m}$  at the southern part of the profile due to the presence of low lying coarse-grained sand. The variation in the resistivity reveals the inhomogeneity along the top layer. This layer is underlain by more conductive layer, which has resistivity values ranges from 220  $\Omega\text{m}$  to 400  $\Omega\text{m}$  and thinned out towards the northern and southern ends of the

profile with considerable thickness between 2 and 3 m. The layer is interpreted as clay/clayey sand. Below this layer is fractured basement with resistivity values ranges from 500  $\Omega\text{m}$  to 800  $\Omega\text{m}$ , which formed the upper section of the basement rock. It has uniform thickness of 6 m across the profile. The base of this profile was occupied by the basement rock, which has resistivity values of 1200  $\Omega\text{m}$  and above. The depth to the basement ranges from 3 m to 13.4 m (Figure 12). The uneven thickness across the profile line indicates that there was no uniform weathering across the profile line (Figure 12).

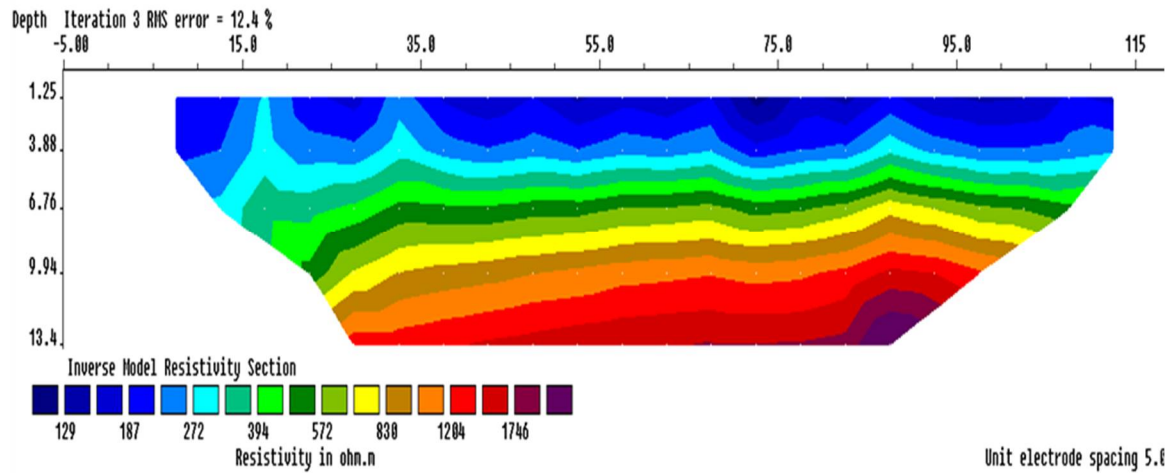


**Figure 12: Inverse model resistivity section for profile 3**

**Profile 4**

The maximum length of inverted section of 2-Dimensional imaging of profile 4 located at the northern section of the study area is 120 m. The upper part of the layer revealed the presence of materials with resistivity values ranging from 120  $\Omega$ m to 400  $\Omega$ m, which was interpreted as sandy clay/lateritic clay. The thickness of the layer varies from less than 1.25 m towards the southern end of the profile to 6 m towards the western end of the profile. The intermediate layer has resistivity values ranging between 450  $\Omega$ m and 800  $\Omega$ m. The materials were

interpreted as clay/clayey sand with thickness varies from 2.5 to 2.8 m. The degree of weathering in this profile is high, resulting in high percentage of the clay/clayey sand in the profile. Beneath this layer is the fresh basement with resistivity ranges from 800  $\Omega$ m to 1072  $\Omega$ m. The upper section of this layer was interpreted as moderately weathered/fractured basement with thickness of about 5 m. The lower part of the layer represents the basement rock, with resistivity above 1300  $\Omega$ m and dips westward (Figure 13).

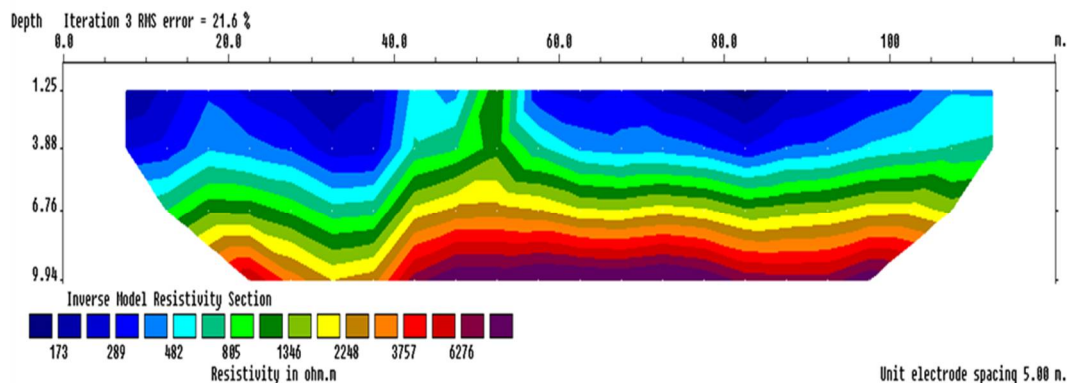


**Figure 13: Inverse model resistivity section for profile 4**

Generally, the distribution of the subsurface soil resistivity in the results (Figures 6 to 14) show a wide variation in the soil resistivity and at different depths along the profiles. The resistivity of the three-layer case reveals that the top layer is characterized with relatively high resistivity across the study site with the resistivity value ranges from 80  $\Omega\text{m}$  to 200  $\Omega\text{m}$  and the thickness varies from < 1.25 to 3 m.

The variations in the resistivity values depict the in-homogeneity nature of the layer. The presence of clayey sand/sandy clay with lateritic clay and occasionally outcrop are responsible for heterogeneity of the subsurface. The intermediate layer is characterized with relatively resistivity values ranging from 300-Ohm-m to 720-Ohm-m and the thickness vary from 3 m to 9 m. The layer is characterized by the dominance of clay/clayey sand (Olayinka *et al.*, 2004). The layer is hydro-geologically good because of the weathered material, which constitutes the layer, has high porosity and contains a significant amount of water, but presents low permeability due to its relatively high clay content (Barker, 2001).

The fractured/fresh basement underlies the main aquiferous zone (unconfined aquifer) with resistivity ranging between 546  $\Omega\text{m}$  to 88674  $\Omega\text{m}$  at VES 6 and VES 9 respectively. The thickness of the fractured basement, which serves as confined aquiferous zones ranges from 4 m to 11.2 m. The overburden thickness varies across the survey area with some portions having thickness above 13.4 m. Geophysical studies in south-western basement complex of Nigeria have identified thick overburden as zones of high groundwater potentials (Olorunfemi and Okhue, 1992; Oladapo *et al.*, 2004; Oyedele and Olayinka, 2012).

Olayinka *et al.* (2004) submitted that weathered/fractured basement with resistivity between 100  $\Omega\text{m}$  and 800  $\Omega\text{m}$  found in the basement complex of Nigeria are good groundwater aquifer. The cusps/drop pattern observed between the layer and basement rock show differential weathering and fracturing in association with gneissic host rock especially near the contact and such areas are hydro-geologically potential site for groundwater reserves and target for groundwater development. According to Louis *et al.* (2002), groundwater favourable areas are locations where the intense fracturing of the basement rock has produced extensive or local thickening of overburden material.

## CONCLUSION

The results show that the basement rock delineated with resistivity is in order of 1000  $\Omega\text{m}$  to 9459.3  $\Omega\text{m}$ . The bedrock topography has a variable thickness of overburden between 3 m and above 16.4 m. The different terrain where the overburden are located can be explored for groundwater development. Electrical resistivity methods have provided information on the lithological units, weathering profiles and geological structures favorable for groundwater exploration and development in the study area. The analyses of the inverted sections along the profiles and VES results interpreted show three divisions viz. topsoil, which is clayey sand/sandy clay/lateritic clay; weathered layer which contains clayey materials and the fractured/fresh basement with the fractured part acting as the aquifer in the area. The aquifer unit in the study area is weathered basement obtained often from in-situ weathered crystalline rocks. The bedrock depressions and the fractured zones are favourable groundwater potential areas because they are collection centers for

groundwater.

The survey presented three layer of H-type and A-type resistivity curve. The H-type curve which is about 33% while the A type is 66%. The geo-electric section revealed three to four major geological formation presences in the study area, which are top-soil, weathered bedrock, fractured/fresh bedrock and clayey weathered bedrock. Fractured bedrock and weathered bedrock within the study area are promising location for possible groundwater exploration. The geophysical survey show that VES 2, VES 3, VES 4, VES 5, and VES 6 are possible location for groundwater extraction.

## REFERENCES

**Ajayi O., Adegoke-Anthony, C.W.** 1988. Groundwater prospects in the basement complex rocks of Southwestern Nigeria. *Journal of African Earth Science*, vol. 7, No.1, pp. 227.

**Anomohanran Ochuko** 2013. Investigation of Groundwater Potential in Some Selected Towns in Delta. *International Journal of Applied Science and Technology* Vol. 3 No. 6; August 2013.

**Ayolabi E. A., Adeoti L., N.A. Oshinlaja N. A., Adeosun I.O., Idowu O.I.** 2009. Seismic Refraction and Resistivity Studies of part of Igbogbo Township, South-West Nigeria. *Journal Sci. Res. Dev.*, 2008 / 2009, Vol. 11, 42 – 61

**Barker, R.D.** 1999. Surface and borehole geophysics. In Lloyd J. W. (ed) *Water Resources*

**Barker, R. D.** 2001. Imaging fractures in hard rock terrain. University of Birmingham, UK. <http://www.bham.ac.uk/>

[EarthSciences/research/hydro/envgeo/](http://EarthSciences/research/hydro/envgeo/)

**Cheng P. H, Ger Y. I., Lee S. L.** 2008. An electrical resistivity study of the Chelungpu fault in the Taichung area, Taiwan, *Terrestrial Atmospheric and Oceanic Sciences* 19 241-255.

**Crook N, Binley A, Knight R., Robinson D A, Zarnetske J ,Haggert R.** 2008. Electrical resistivity imaging of the architecture of substream sediments, *Water Resource Res.* 44 W00D13.doi:10.1029/2008WR006968.

**Geo-Etude** 2003. Rural water supply program in Ghana; Resistivity and Induced polarisation imaging survey. *Technical report* no. R588-02.

**Griffiths, D. H., Barker R. D.** 1993. Two-dimensional resistivity imaging and Modeling in areas of complex geology, *Journal of Applied Geophysics.* 29 211–226.

**Hauck C., Muhll D. V., Maurer H.** 2003. Using DC resistivity tomography to detect and characterize mountain permafrost. *Geophysical Prospecting.* 51 273-284.

**Hsu H., Yanites B J., Chihchen C., Chen Y,** 2010. Bedrock detection using 2D electrical resistivity imaging along the Peikang River, Central Taiwan, *Geomorphology.* 114 406-414.

**Jayeoba, A., Oladunjoye, M.A.** 2015. 2-D Electrical Resistivity Tomography for Groundwater Exploration in Hard rock Terrain. *International Journal of Science and Technology* vol. 4(4).

**Jones, H. A., Hockey, R. D.** 1964. *The geology of parts of Southwestern Nigeria.* *Geology. Survey Niger. Bull.* 31: 22-24.



- Keller, G.V. and Frischknecht, F.C.** 1966. *Electrical Methods in Geophysical Prospecting*. Pergamon Press, Oxford.
- Lawrence, A. O, Ojo T. A.** 2012. The use of Combined Geophysical Survey Methods for Groundwater Prospecting in a Typical Basement Complex Terrain: Case Study of Ado-Ekiti Southwest Nigeria, *Research Journal in Engineering and Applied Sciences* 1(6): 362-376.
- Louis, I. F., Louis, F. I., Grambes, A.** 2002. Exploring for favourable groundwater conditions in hard rock environments by resistivity imaging methods: synthetic simulation approach and case study example, *International conference on Earth's Sciences and Electronics. Special issue*, 1-4.
- Loke, M. H.** 2000. Electrical imaging surveys for environmental and engineering studies, a practical guide to 2-D and 3-D surveys. 6P, 2000.
- Loke, M. H.** 2004. Tutorial: 2-D and 3-D electrical imaging surveys, *www.geoelectrical.com*, version December 2013.
- NIMET.** 2011. Nigerian Metrological Agency, *daily weather guide*. Nigeria Television Authority, Lagos, Nigeria.
- Okafor Pudentiana Ngozi,** 2011. Integration of Geophysical Techniques for Groundwater Potential Investigation in Katsina-Ala, Benue State, Nigeria. Thesis Submitted to the Department of Geology, Faculty of Physical Sciences, University of Nigeria, Nsukka, Nigeria.
- Oladapo M. I, Mohammed M. Z., Adeoye O. O., Adetola B. A,** 2004. Geoelectric investigation of the Ondo state housing corporation estate, IjapoAkure, southwestern Nigeria, *Journal of Mining and Geology*, 40 (1) 41-48.
- Olayinka, A. I., Amidu, S. A., Oladunjoye M. A.** 2004. Use of electromagnetic profiling and resistivity sounding for groundwater exploration in the crystalline basement area of Igbeti, southwestern Nigeria, *Global journal of Geological sciences*, 2 (2) 243-253.
- Olorunfemi, M. O. Okhue ,E. T.** 1992. Hydrogeological and Geologic significance of a geo-electric survey at Ile-Ife, *Nigeria Journal of Mining and Geosciences Society*. 28 221-229.
- Oyedele E. A and Olayinka A. I.** 2012 Statistical evaluation of groundwater potential of Ado-Ekiti southwestern Nigeria, *Transnational Journal of Science and Technology*. 2 (6) 110-127.
- Rahman M. A.** 1989. Review of the Basement Geology of Southwest, Nigeria. *Geology of Nigeria* pp. 943-959.
- Rao, B. V., Prasad, Y. S., Reddy, K. S.,** 2013. Hydrogeophysical investigations in a typical Khondalitic terrain to delineate the kaolinised layer using resistivity imaging, *Journal Geological Society of India*. 81 521-530.
- Sharma, S. P., Baranwal, V. C.,** 2005. Delineation of groundwater-bearing fracture zone in a hard rock area integrating Very Low Frequency electromagnetic and resistivity data, *Journal of Applied Geophysics*. 57 155-166.
- Sundaravaradan, N.A., Reddy Bharata M. Jaya** 2018. How is Earthing done?. *IEEE Potentials* 37(2): 42-46.

- 
- Yang C. H. Chang P. H., You J. I., Tsai L. L.** 2002. Significant resistivity changes in the fault zone associated with the 1999 Chi-Chi earthquake, west central Taiwan, *Tectonophysics*. 350 299-313
- Zhou, Q. Y., Matsui H., Shimada, J** 2004. Characterization of the unsaturated zone around a cavity in fractured rocks using electrical resistivity tomography, *Journal Hydraulic Res.* 42 25-31.

*(Manuscript received: 8th April, 2019; accepted: 11th March, 2020)*